Geomechanics and Engineering, *Vol. 23, No. 6 (2020) 523-533*
DOI: https://doi.org/10.12989/gae.2020.23.6.523

End shape and rotation effect on steel pipe pile installation effort and bearing resistance

Muhammad A. Saleem[a], Adnan A. Malik* and Jiro Kuwano[b]

Department of Civil and Environmental Engineering, Saitama University, 255 Shimo-Okubo, Sakura-ku, Saitama-shi, Saitama 338-8570, Japan

(Received June 17, 2020, Revised December 3, 2020, Accepted December 11, 2020)

Abstract. The current study focuses on the effect of the end shape of steel pipe piles on installation effort and bearing resistance using the pressing method of installation under dense ground conditions. The effect of pile rotation on the installation effort and bearing resistance is also investigated. The model steel piles with a flat end, cone end and cutting-edge end were used in this study. The test results indicated that cone end pile with the pressing method of installation required the least installation effort (load) and showed higher ultimate resistance than flat and cutting-edge end piles. However, pressing and rotation during cutting-edge end pile installation considerably reduces the installation effort (load and torque) if pile penetration in one rotation equal to the cutting-edge depth. Inclusion of rotation during pile installation reduces the ultimate bearing resistance. However, if penetration of the cutting-edge end pile equal to the cutting-edge depth in one rotation, the reduction in ultimate resistance can be minimized. In comparing the cone and cutting-edge end piles installed with pressing and rotation, the least installation effort is observed in the cutting-edge end pile installed with penetration rate equal to the cutting-edge depth per rotation.

Keywords: steel pipe pile; pile end shape; installation effort; pressing and rotation; dense sand

1. Introduction

Deep foundations or pile foundations are used to transfer the structural load to the firm stratum at deeper depth when ground surface soil at shallow depth does not have sufficient bearing capacity to support structural load (Budhu 2010). The material of the pile can be concrete, steel, timber, plastic, or composite. Its selection depends on material availability, the magnitude of loading, type of soil, and site conditions in which the pile is installed (Budhu 2010). Driven piles are generally installed with impact driving, vibro-driving, pressing, and a combination of pressing and torque. These installation methods have a different effect on the surrounding ground and the ultimate resistance of the pile. Based on centrifuge modelling and material point method, jacked piles' installation mechanics densify the surrounding ground and increase the bearing resistance in loose and medium dense sand (Phuong *et al.* 2016). In the case of impact driving, true energy ratios (65% and 98%) during driving of the steel or driven cast-in-situ piles are strongly dependent on hammer drop height. The ground conditions significantly affect the energy ratio for a given drop height (Flynn and McCabe 2019). Pipe piles installed with vibro-driving compact wider area than impact driving (Daryaei *et al.* 2020). Much research has been conducted on the axial capacity of driven piles in dense sand. However, it is still the most arguable area with high uncertainty in foundation design (Randolph *et al.* 1994). Steel pipe piles can be open-ended and close-ended. As many researchers investigated, open-ended piles' behavior is different from close-ended piles (Randolph *et al.* 1979, Paikowsky and Whitman 1990, Lee *et al.* 2003, Paik *et al.* 2003). The installation effort required to install the open-ended pile is less than close-ended pile under similar ground conditions (Paik *et al.* 2003). The installation method is also an essential factor in driving resistance of open and close-ended piles (McCammon and Golder 1970, Lu 1985, Smith *et al.* 1986, Brucy *et al.* 1991). According to Paik *et al.* (2003), open-ended piles driven in plugged mode perform similarly to close-ended piles. The normalized unit base resistance and unit shaft resistance of open-ended piles are less than close-ended piles. A previous study stated that both the dynamic load test and static load test showed comparable values for driven piles in loose and dense sand (Heins *et al.* 2020). According to Kumara *et al.* (2016), open-ended pile wall thickness affects the soil plug height. Moreover, a thinner-walled pile produces a higher degree of soil plug at greater depth. In open-ended piles, the incremental filling ratio (IFR) changes with change in the installation method and the soil state. Moreover, open-ended piles' group capacity increases with an increase in IFR (Fattah *et al.* 2018). The hybrid computational intelligence technique (FA-ANFIS) without considering the internal friction angle and unit weight of the soil showed the best results for driven pile (open-ended and steel H) capacity prediction (Sun *et al.* 2020).

The advancement in installation techniques has significantly increased the usage of driven piles. Nowadays,

*Corresponding author, Assistant Professor, Ph.D.
E-mail: adnanmalik@mail.saitama-u.ac.jp
[a]M.Eng Student
[b]Professor

Copyright © 2020 Techno-Press, Ltd.

ISSN: 2005-307X (Print), 2092-6219 (Online)

piles can be driven with minimum noise and vibration that further enhances the driven pile acceptability even in urban areas. Pressing is one of the methods which produce less noise and vibration during the installation of the pile. The pressing method (press-in) of installation with rotation showed a good agreement between estimated and measured base resistance for close-ended piles (Ishihara *et al.* 2015). This method of installation is used nowadays for both open-ended and closed-ended piles. The previous study indicated that open-ended piles' performance at greater depth is comparable with close-ended piles (Klos and Tejchman 1981, Yang *et al.* 2020). It was investigated through acoustic emission that driving of close-ended pile can cause sand particles breakage in the shear zone area. Moreover, the sand below the pile tip, i.e., within the compression zone, showed insignificant breakage (Mao *et al.* 2020). According to Ni *et al.* (2017), the pipe pile (cone end) with drainage holes within the bottom 50% of pile length dissipates the excess pore pressure more quickly in clays. The end condition of circular, square, and H displacement piles have no visible effect on P-y response at z/B<3 under 1 g and centrifuge tests in soft clay (Truong and Lehane 2018).

The pile should be installed deeper until a competent stratum is found to achieve higher bearing resistance. In order to reach such a competent stratum, the installation effort (pushing force, torque) should be controlled in a manner that it should not exceed the installation machinery capacity. The installation effort not only depends upon the initial density of the ground but also on the geometry of the pile, pile end shape, end condition (open or closed), installation method, etc. In the light of previous studies, the current study focuses on the steel pipe pile's end shape (close-end) effect on installation effort and bearing resistance in dense sand. Moreover, the effect of end shape on the state of the surrounding ground is also investigated. Also, the effect of rotation during the installation of the pile on the installation effort and bearing resistance is studied. Model scale piles with different end shapes, i.e., flat end, cone end, and cutting-edge end, are considered in this study.

2. Testing equipment

A hollow steel pipe having a diameter (D_S) of 21.7 mm was used as a model steel pipe pile in this study, as shown in Fig. 1(a). The pile length was 600 mm. Three different types of pile end shapes, i.e., flat end, cone end, and cutting-edge end, were used as shown in Fig. 1(a). Recently, cutting-edges are used in practical field to reduce the installation effort. However, the dimensions of these cutting-edges are not documented. Therefore, in this study, an attempt is made to check the benefit of using cutting-edge end pile on installation effort and bearing resistance. As a start off, the cutting-edge depth (CED) was considered as 3.8 mm, i.e., $D_S/5.71$ or $CED/D_{50} = 19$. In addition, the inclined length of cutting-edge to median particle size (D_{50}) ratio of 27 was used, which is more than the minimum recommended particle scaling ratio used in DEM simulation (Arroyo *et al.* 2011, Sharif *et al.* 2020). Dimension details of the pile end shapes are available in Fig. 1(a). The bottom strain gauges on the pile were used to record the strain reduction due to the surrounding soil (Fig. 1(c)). This strain was converted to load (P_B = Young's Modulus x Strain x Area of the hollow shaft). The top strain gauges were used to record the strain load above the soil. The strain load difference between the top and bottom strain gauges was due to the soil-pile shaft interaction, termed as skin friction. The obtained skin friction was subtracted from the top strain gauge load to estimate the end bearing resistance. In order to verify the response of strain gauges, calibration was made before and after the pile load test without the presence of surrounding ground. Two load cells were used for the calibration. One load cell was placed on top of the pile, while another load cell was placed under the pile tip (Fig. 1c). It was made sure that the load on top of the pile, under the tip, on top strain gauges, and bottom strain gauges was similar. A similar strain gauge configuration was also used by Nagai *et al.* (2018).

A steel container having a diameter of 1000 mm with a depth of 1100 mm was used to prepare the model ground, as shown in Fig. 1(b). In the model-scale testing, the size of the model container is critical. It should be with respect to the pile diameter; otherwise, the test results will be affected by the boundary conditions. As per the previous studies, the zone around the pile affected by the load is 1.5 to 2.5 times the pile diameter. Below the pile, it is 3.5 to 5.5 times the pile diameter in clean sand (Yang 2006). Malik *et al.* (2019, 2020) used a container size of 600mm and model piles with a diameter of 21.7 to 89.1 mm and found that the container size is adequate with respect to pile diameter. To avoid the boundary effects, the radius of the soil chamber should be more than 20 times the radius of the pile (Bolton *et al.* 1999). Moreover, according to Sharif *et al.* (2020), the mean effective stress along depth does not change significantly after a radial distance of 20 times the pile radius. Hence, one can believe that the results are not affected by the boundary of the container. In the present study, clearance around the pile was 23 times the pile shaft diameter (D_S). Clearance below the pile tip was 27.5 times the pile shaft diameter, as shown in Fig. 1(b). Toyoura sand in a dry state was used to develop the model ground. The relative density (RD) of the model ground was kept at approximately 70%. The properties of Toyoura sand are as follows; specific gravity = 2.65, D_{50} (50% pass particle size) = 0.20 mm, e_{max} (maximum void ratio) = 0.98 and e_{min} (minimum void ratio) = 0.60. In a model-scale test, the size of the buried structure should be 48 times greater than D_{50} value to eliminate the size effect (Ovesen 1981, Dickin and Leung 1983, Abdoun *et al.* 2008). In this work, the diameter of the pile is 21.7 mm, and the D_{50} value is 0.2 mm. Hence, one can believe that the results are not affected by the size of the pile and the soil. The displacement control loading system was used to install the pile. A rotation system was used to rotate the pile during installation. Load and torque were monitored during installation of the pile with the help of a load/torque transducer (for load: capacity = 25 kN, sensitivity = 0.11 strain/N for torque: capacity = 500 Nm, sensitivity = 3.92 strain/Nm). The pile penetration during installation and pile load test was measured with displacement transducer (capacity = 500 mm, sensitivity = 20 strain/mm), as shown in Fig. 1(b). The data logger was used to record all the data.

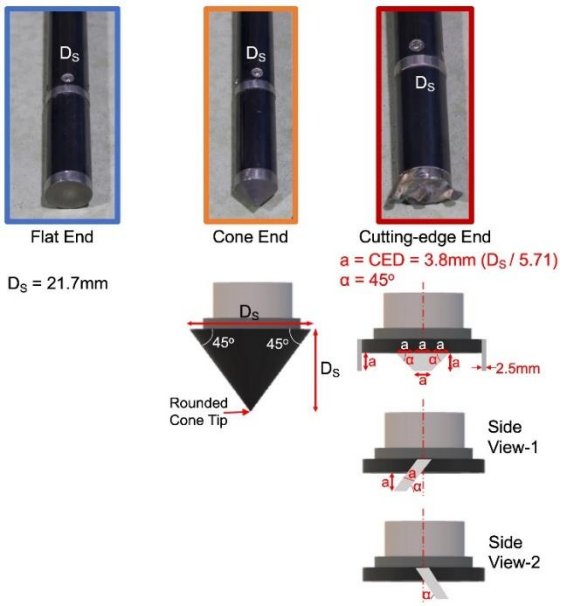

(a) Different pile end shapes

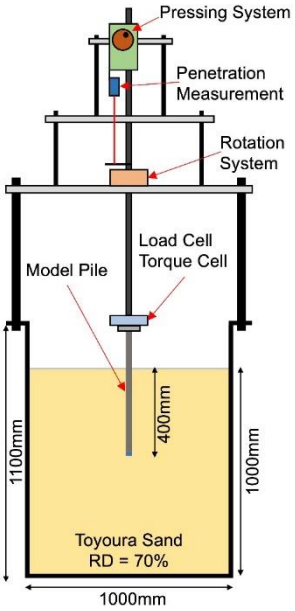

(b) Schematic illustration of testing equipment

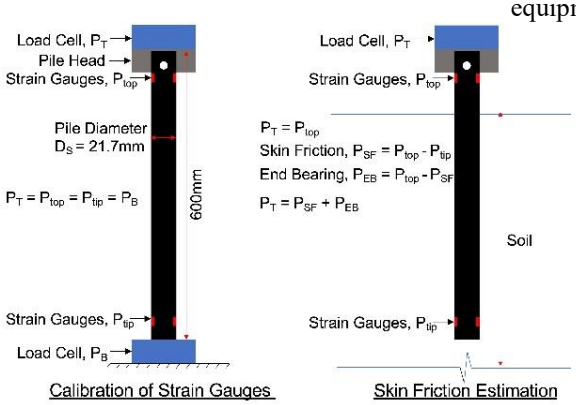

(c) Model steel pipe pile

Fig. 1 Model testing equipment used in this study

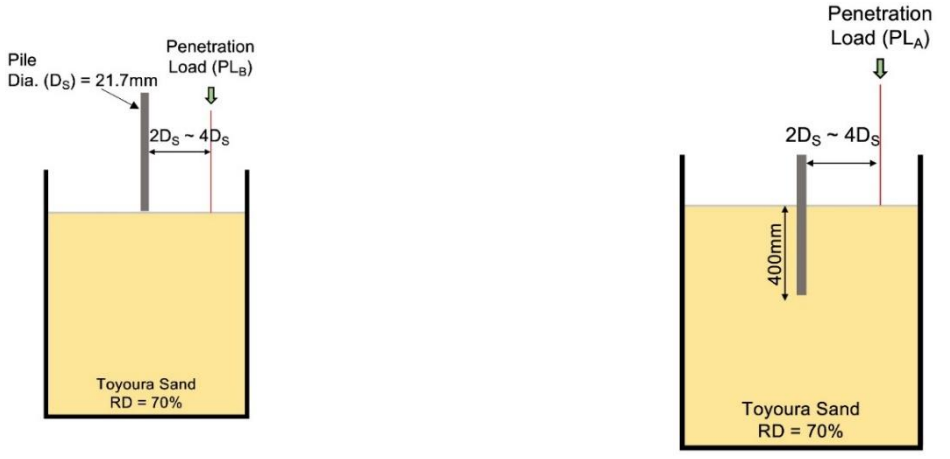

(a) Before installing the pile (b) After installing the pile

Fig. 2 Assessment of model ground state before and after model pile installation

3. Testing methodology

The ground was prepared in the model container in five layers, each having a thickness of 200 mm after compaction. The compaction was done with a rammer. The relative density (RD) of the ground in each layer was

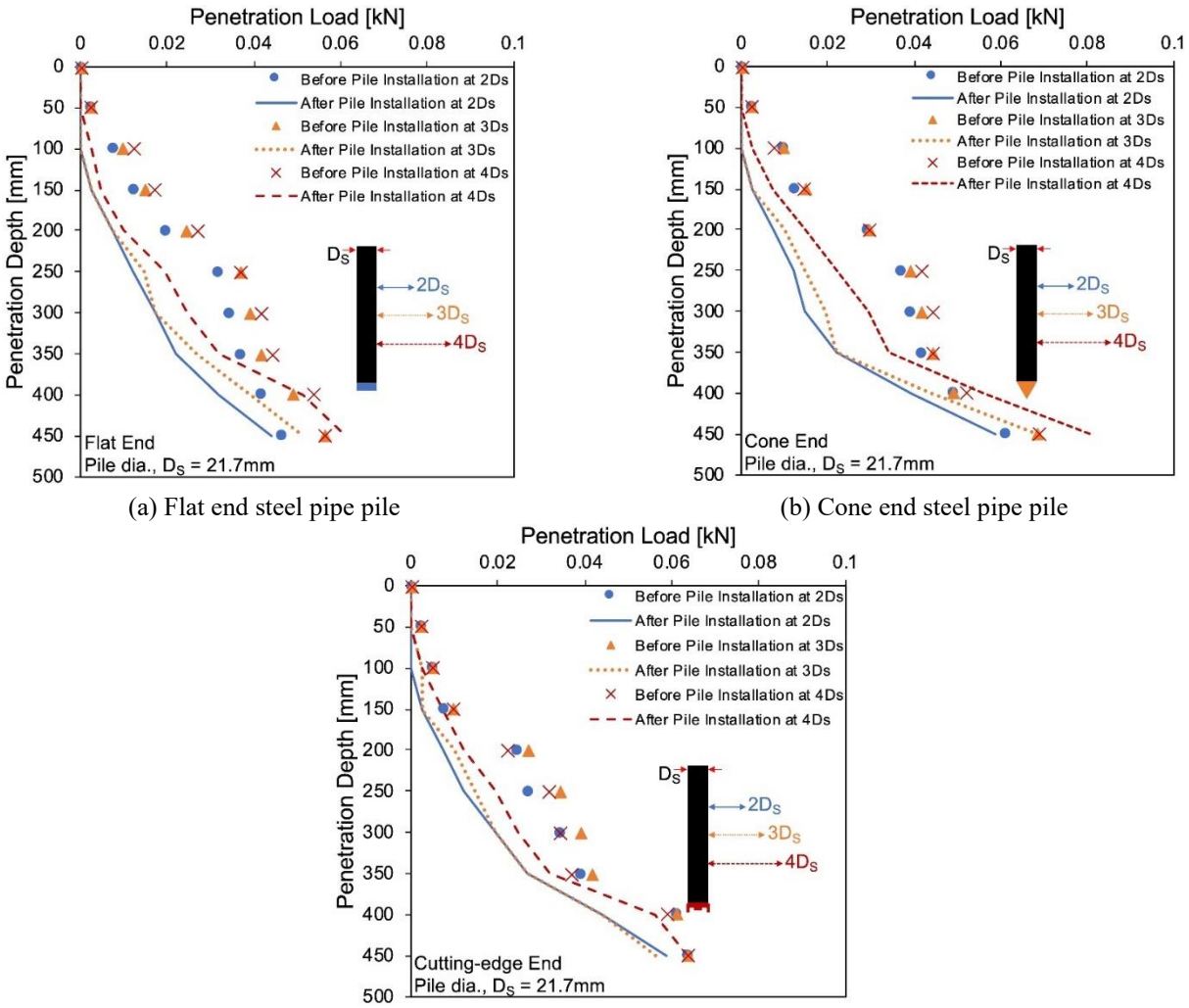

(a) Flat end steel pipe pile

(b) Cone end steel pipe pile

(c) Cutting-edge end steel pipe pile

Fig. 3 State of the surrounding ground after the pile installation

approximately 70%. The compacted depth of the model ground was 1000 mm. The ground's initial state was checked by inserting a thin steel needle having a diameter of 3 mm into the model ground. The penetration load (PL_B) was recorded during the insertion of the needle at a distance of $2D_S$, $3D_S$, and $4D_S$ from the edge of the pile shaft, as shown in Fig. 2(a). After that, the model pile with different end shapes was installed into the model ground by pressing method. The pressing rate considered to install the model steel pipe piles was 15 mm/min. The cone and cutting-edge end piles were installed with pressing and rotation to check the effect of rotation on the installation effort and bearing resistance. The pile was installed up to an embedment depth (E_d) of 400 mm, i.e., E_d/D_S = 18.4. The state of the model ground was again checked by inserting a thin steel needle with a diameter of 3 mm into the model ground after pile installation. The penetration load (PL_A) was recorded again during the insertion of the needle at a distance of $2D_S$, $3D_S$, and $4D_S$ from the edge of the pile shaft, as shown in Fig. 2(b).

After that, the pile load tests were conducted with different pile end shapes. A loading rate of 2 mm/min was considered in a pile load test.

4. Results and discussions

4.1 Installation of pile by pressing method

In this test series, piles with different end shapes were installed by the pressing method. Ishihara *et al.* (2015) used penetration to pile diameter ratio of 4.3 per minute (1380 mm/min) to install the close-ended tubular pile in full-scale testing. Ishihara and Haigh (2018) checked the effect of penetration rate (120, 720, and 1800 mm/min) on the close-ended tubular pile performance (full-scale test). It was found that the base resistance during pile installation reduced with an increase in penetration rate. Moreover, Liu *et al.* (2020) used a 15 mm/min penetration speed to study the effect of flat and cone-ended piles (model-scale test) on ground disturbance. Based on these studies, a penetration rate of 15mm/min (penetration to pile diameter ratio of 0.69) was considered in this work. This penetration rate isslow enough to eliminate the effect of loading rate on the installation load, which is required to study only the impact of pile end shape and rotation on the installation effort. The surrounding ground state was checked before and after the installation of piles. According to ASTM standard D1143,

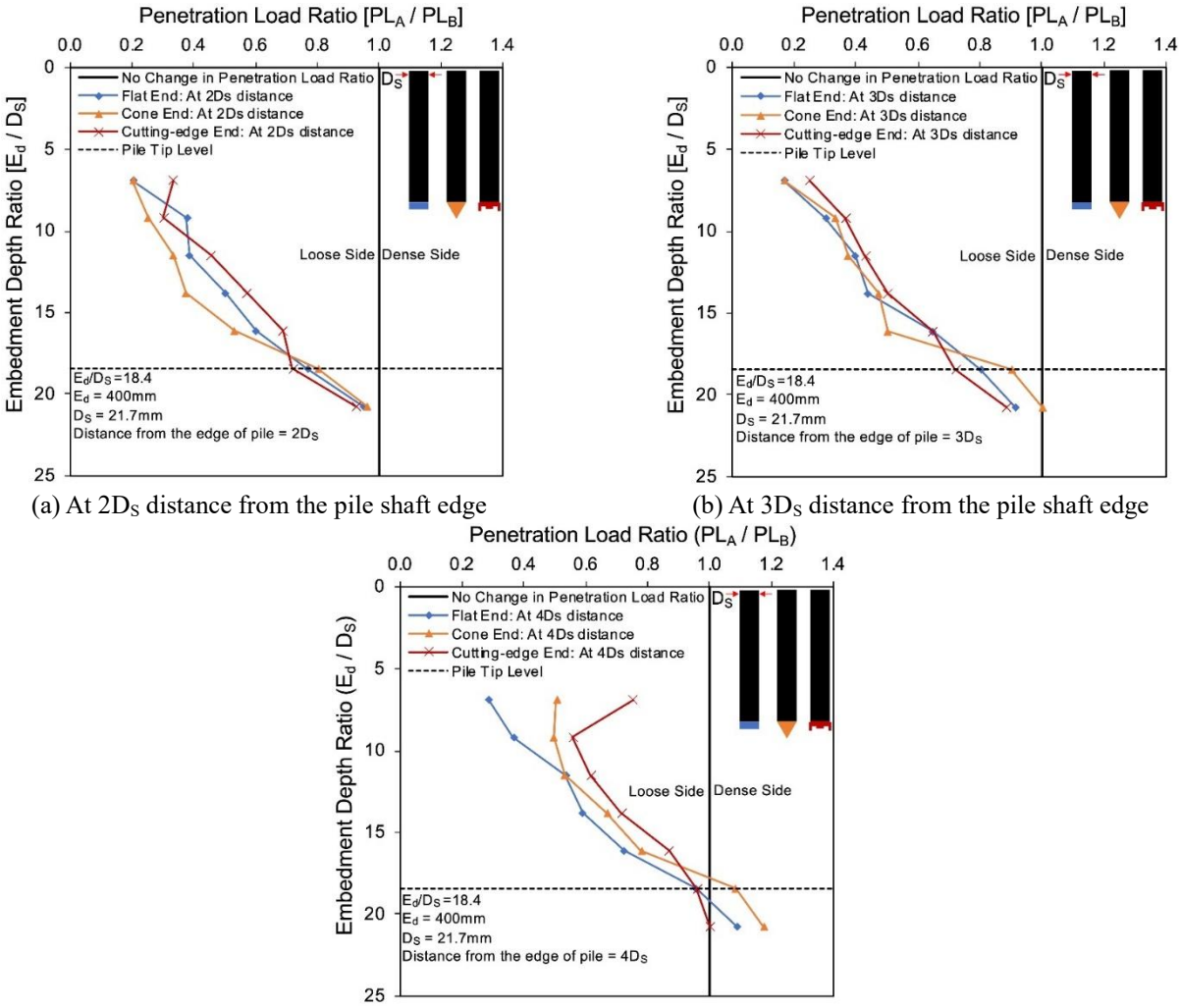

(a) At $2D_S$ distance from the pile shaft edge (b) At $3D_S$ distance from the pile shaft edge

(c) At $4D_S$ distance from the pile shaft edge

Fig. 4 Effect of pile end shape on the state of surrounding ground

the constant penetration rate during pile load test in granular soils should be between 0.75 to 2.5 mm/min. Therefore, in this study, a loading rate of 2 mm/min was considered during the pile load test.

4.1.1 Effect of pile end shape on the state of surrounding ground

The ground state was checked before and after installing the pile at a distance of $2D_S$, $3D_S$, and $4D_S$ from the edge of the pile shaft. The comparison of penetration load before and after the pile installation (for all cases, i.e., flat end, cone end, cutting-edge end) is shown in Figs. 3(a)-3(c). The test results indicated that the difference of penetration load before and after pile installation is high between penetration depth of 250 mm and 350 mm (E_d/D_S = 11.5~16.1), and it is low, below 400mm penetration depth in all the test cases as shown in Figs. 3(a)-3(c). Moreover, the overall difference of penetration load before and after pile installation is high close to the pile (at $2D_S$ distance), and it became low away from the pile (at $4D_S$ distance) as shown in Figs. 3(a)-3(c). The disturbance zones around the pile can be divided into five regions, i.e., (1) shear slide zone or smear zone, (2) compression zone, (3) transition zone, (4) stress relaxation zone, (5) surface uplift zone based on previous studies (Yang *et al.* 2010, Massarchand and Wersall 2013, Arshad *et al*. 2014, Liu *et al.* 2020). The region (stress relaxation zone) around and above the pile tip includes soil movement in an obliquely upward direction. The direction of movement of displaced soil also depends upon the stress level, i.e., vertical soil displacement is more near the surface. Based on these, it is presumed that the disturbance between 250 mm and 350 mm falls in the zone where displaced soil movement is dominant in the horizontal direction. However, the stress level is not enough to restrict the vertical soil movement, which results in more ground disturbance. This disturbance gradually decreased as the stress level increased.

The ground state change due to pile installation is represented as the penetration load ratio (PLR). It is a ratio between measured penetration load after installation (at a distance of $2D_S$, $3D_S$, $4D_S$ from the edge of the pile) to measured penetration load before installation, and it is represented as;

$$PLR = \frac{PL_A}{PL_B} \quad (1)$$

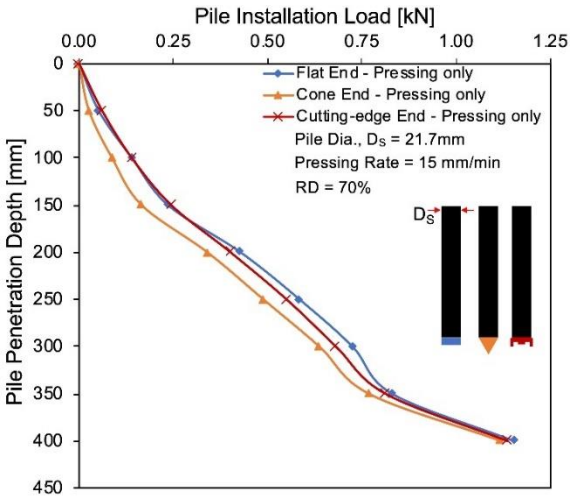

Fig. 5 Effect of pile end shape on the installation effort

PLR= Penetration load ratio, PL_A= Penetration load measured after the installation of pile (kN), PL_B= Penetration load measured before the installation of pile (kN), PLR=1 (no change in the state of the ground), PLR>1 (densification of the ground), PLR<1 (loosening of the ground)

The test results indicated that the ground state changed in all the test cases with different end shapes, as shown in Figs. 4(a)-4(c). It is observed that steel pipe piles with a flat end, cone end, and cutting-edge end loosen the dense ground, especially above the pile tip level, i.e., <400 mm or E_d/D_S = <18.4. The cutting-edge end pile produced the least disturbance (loosening) along the pile length in the ground at $2D_S$, $3D_S$, and $4D_S$ distance (away from the pile), as shown in Figs. 4(a)-4(c). However, minimal change in the ground state is observed below the pile tip level, i.e., >400mm or E_d/D_S = >18.4. The cone end pile produced the least disturbance (loosening/densification) below the pile tip at $2D_S$, $3D_S$, and $4D_S$ distance (away from the pile), as shown in Figs. 4(a)-4(c). Moreover, at a distance of $4D_S$ (away from the pile edge), the cone end pile showed 17% densification, whereas the flat end pile showed 9%. The cutting-edge end pile did not disturb the ground, as shown in Fig. 4(c). According to Liu *et al.* (2020), the shear slide zone or smear zone is quite thin, and its characteristics are similar in the flat end and cone end piles. The main difference in the soil displacement under flat end and cone end piles is the absence of a meta-stable sand plug under the cone end pile. Thus, the extent of the transition zone is more under cone end pile than flat end and cutting-edge end piles. The soil movement in the transition zone is radial with an inclination in an upward direction. It is presumed that due to the greater extent of the transition zone under the cone end pile, the ground is more disturbed above the pile tip than the flat end and cutting-edge end piles, whereas the ground is more densify below the pile tip due to the greater extent of the transition zone under the cone end pile. Moreover, according to Melnikov and Boldyrev (2014), a compaction zone exists under cone end pile at four times the pile diameter distance away from the pile. Based on these observations, it is presumed that densification occurred below the pile tip.

4.1.2 Effect of pile end shape on the installation effort

Steel pipe piles with a flat end, cone end, and cutting-edge end were installed in the dense model ground by pressing method (compressive loading). A pressing rate of 15 mm/min was considered while installing the pile. The pile was installed up to an embedment depth of 400 mm. The test results indicated that overall steel pipe pile with cone end required the least installation effort (installation load) than flat end and cutting-edge end piles, as shown in Fig. 5. The flat and cutting-edge end piles required more or less similar installation effort to reach an embedment depth of 400 mm, i.e., E_d/D_S = 18.4. In comparison between cutting-edge and flat end piles, the flat end pile showed a higher installation load from 200 mm to 350 mm (E_d/D_S, 9 to 16) depth of installation, as shown in Fig. 5.

4.1.3 Effect of pile end shape on the bearing resistance

After installing the pile using the pressing method, the pile load test was conducted on the steel pipe piles with a flat end, cone end, and cutting-edge end. A loading rate of 2 mm/min was considered during the pile load test. It is observed that total pile resistance, i.e., end bearing resistance and skin resistance, of cone end pile is higher than flat end and cutting-edge end piles, as shown in Fig. 6(a). The ultimate resistance (considered at plunging resistance state) of cone end pile is 5.6% higher than flat end pile and 5.9% higher than cutting-edge end pile, as shown in Fig. 6(a). However, if total resistance is distributed into end bearing and skin resistance, then skin resistance is higher in cutting-edge end pile, whereas end bearing is higher in cone end pile, as shown in Fig. 6(b). The increase in skin resistance in cutting-edge end pile is due to less ground disturbance (loosening of the ground) from others (flat and cone end) along the length of the pile during the installation of the pile (refer Fig. 4). The increase in end bearing in cone end pile is due to less ground disturbance (loosening/densification of the ground) from the others (flat and cutting-edge end) at and below pile tip level during the installation of the pile (refer Fig. 4). The ultimate skin resistance (considered at plunging resistance state) of the cutting-edge end pile is 72.7% higher than the cone end

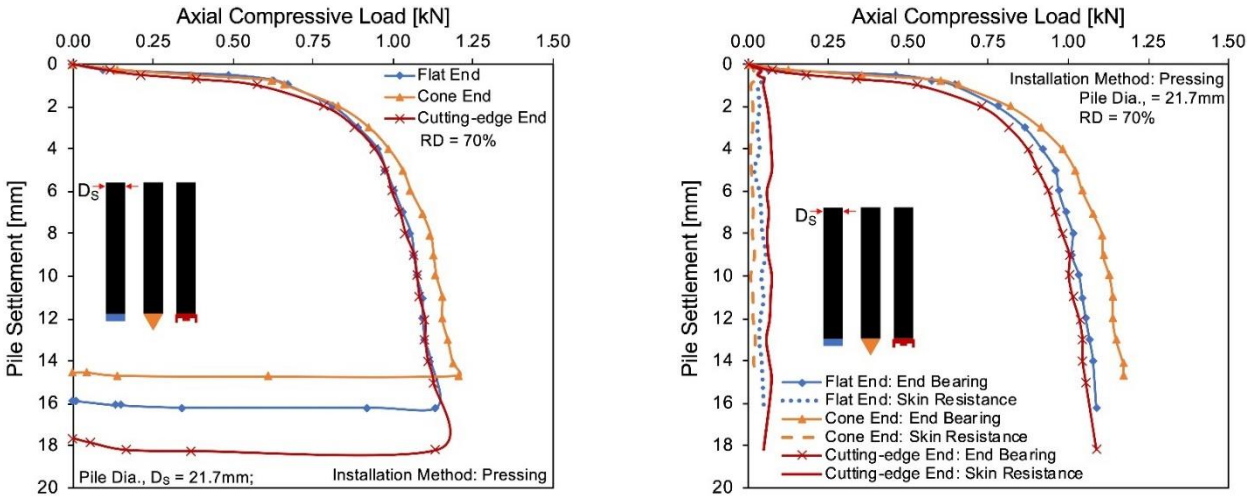

(a) Ultimate load settlement behavior (b) End bearing and skin resistance

Fig. 6 Pile load test on steel pipe piles with flat end, cone end, and cutting-edge end

pile and 38.0% higher than the flat end pile, whereas end bearing resistance (considered at plunging resistance state) of the cone end pile is 10.2% higher than the cutting-edge end pile and 7.7% higher than the flat end pile. In this test series, the range of end bearing contribution is 93 to 98%. It is also observed that the maximum pile installation load achieved at the penetration rate of 15mm/min is quite close to the ultimate bearing capacity of the pile (pile load test rate, 2 mm/min). This indicates that the pile installation rate is not affecting the bearing capacity of the displacement pile.

4.2 Installation of pile by pressing and rotation

In this test series, piles with cone and cutting-edge end shapes were installed by pressing and rotation. A pressing rate of 15 mm/min was kept in all the tests. The model ground was compacted at a relative density (RD) of approximately 70%. The pile was installed up to an embedment depth of 400 mm, i.e., E_d/D_S = 18.4. A loading rate of 2 mm/min was considered during the pile load tests. Rotation speed of 0.0263, 0.1315, 0.2105, and 0.2631 rotation/mm were considered in this test series. The selection of rotation speed was based on the cutting-edge depth (CED), i.e., 3.8 mm (refer Fig. 1(a)), and it is related to the penetration of 3.8 mm (CED) into the ground per rotation. The relationship between rotation speed and cutting-edge depth is given below;

• Rotation speed during pile installation = 0.0263 rotation/mm

• Embedment depth, E_d= 400 mm

• Total number of rotations during pile installation = 0.0263 x 400 = 10.52 rotations

• Cutting-edge Depth, CED (refer Fig. 1(a)) = 3.8 mm

• Penetration of pile in one rotation, L_P = 400 / 10.52 = 38.0 mm = 10 x 3.8 = 10 x CED

Similarly,

• Rotation speed = 0.1315 rotation/mm; Penetration of pile per rotation = 7.60 mm = 2.0 x CED

• Rotation speed = 0.2105 rotation/mm; Penetration of pile per rotation = 4.75 mm = 1.25x CED

• Rotation speed = 0.2631 rotation/mm; Penetration of pile per rotation = 3.80 mm = 1.0 x CED

4.2.1 Effect of cutting-edge end shape on the installation effort

Inclusion of rotation in press-in installation method reduced the vertical installation force (White *et al.* 2010, Frick *et al.* 2018, Sharif *et al.* 2020). According to Sharif *et al.* (2020), the installation pitch (p) should be greater than 8 to reduce the installation force and torque. The installation pitch (Eq. (2)) is the ratio between vertical and rotational velocity. In this study, a steel pipe pile with a cutting-edge end was installed by pressing and rotation. The rotation speed was varied from 0.0263 (p = 1.8) to 0.263rotation/mm (p = 17.9). The selection of rotation speeds was based on the whole cutting-edge penetration, i.e., 3.8 mm in one rotation (refer to section 4.2 for details).

$$p = \frac{\dot{\theta} D_S}{2\dot{w}} \quad (2)$$

where, p is installation pitch, $\dot{\theta}$ is rotation speed (rad/s), D_S is pile diameter, $\dot{w}$ is vertical speed (m/s).

Test results indicated that the installation load decreased with an increase in rotation speed, as shown in Fig. 7(a). In terms of cutting-edge depth (CED), minimum installation load is observed when penetration of the pile in one rotation equals the cutting-edge depth (CED = 3.8 mm), i.e., 1.0 x CED. Test results also indicated that the installation torque increased with an increase in rotation speed, except for rotation speed of 0.2631 rotation/mm (1.0 x CED), which showed lesser torque than 0.1315 and 0.2105 rotation/mm, as shown in Fig. 7(b). These results showed that installation effort, i.e., installation load and torque, could be reduced or minimized if penetration of the pile in one rotation equals the cutting-edge depth (1.0 x CED). Therefore, it is suggested that the penetration of the pile in one rotation should be equal to cutting-edge depth.

Test results also indicated that the installation load (P_I) times the penetration per rotation (L_p) to torque (T_I) ratio,

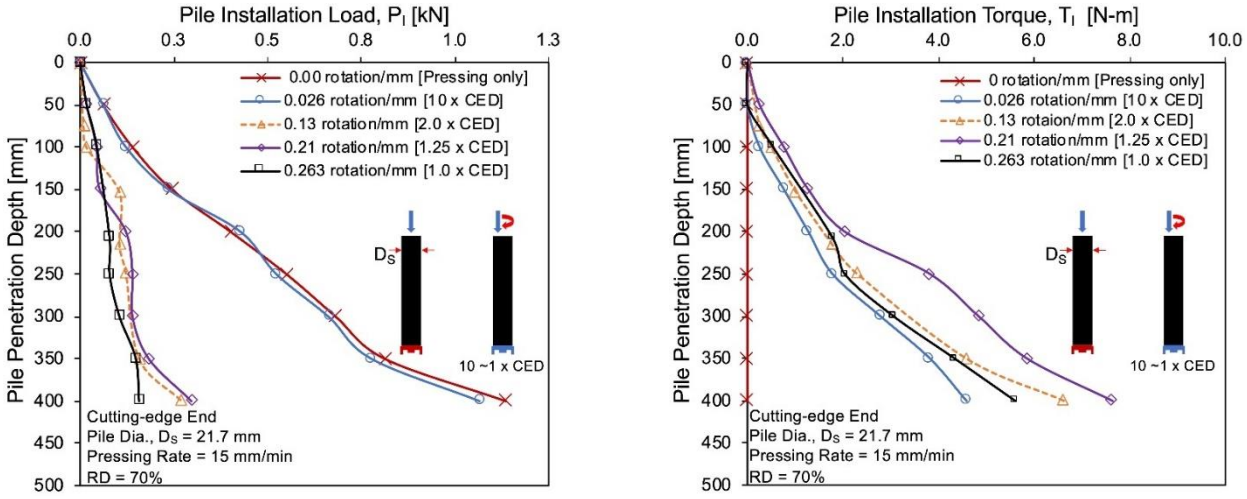

(a) Effect of installation load, P_I (b) Effect on installation torque, T_I

Fig. 7 Relationship of installation effort (load and torque) with rotation speed and cutting-edge depth

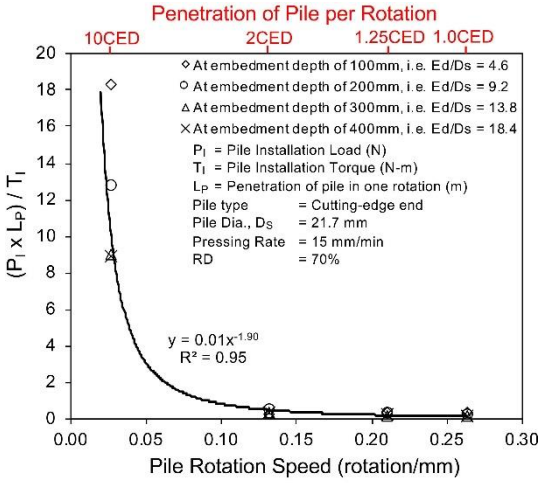

Fig. 8 Relationship of rotation speed with installation load to torque ratio times the penetration per rotation

i.e., $(P_I \times L_P)/T_I$, decreased as a power function (Eq. 3) with an increase in rotation speed (R_S), as shown in Fig. 8. The least ratio is observed at 1.0 x CED, i.e., when penetration of the pile in one rotation equals the cutting-edge depth.

$$\left(\frac{P_I \times L_P}{T_I}\right) = 0.01{R_s}^{-1.90} \quad (3)$$

where,

P_I=Installation load (N), L_P = Penetration per rotation (m), T_I = Installation torque (Nm), R_S = Pile rotation speed (rotation/mm)

4.2.2 Effect of cutting-edge end shape on the ultimate resistance

Test results indicated that the ultimate resistance of pile decreased with an increase in rotation speed. However, the difference between axial compressive loads at higher installation speeds became less, as shown in Fig. 9(a). It is observed that the ultimate resistance of the press-in pile (at plunging resistance state) is almost equal to the pile installed with press-in and rotation at penetration speed equal to the cutting-edge depth in one rotation (1.0 x CED), as shown in Fig. 9(a). The ultimate pile resistance considered at settlement equals 15% of pile diameter decreased with an increase in the rotation speed, as shown in Fig. 9(b). However, in the case of a pile installed with penetration equal to the cutting-edge depth in one rotation (1.0 x CED), the ultimate pile resistance increased by 2%, as shown in Fig. 9(b). The load difference between no rotation case and 1.0 x CED case becomes very close at higher pile settlement, as shown in Fig. 9(b). These results indicated that rotation speed reduces the pile's ultimate resistance in dense ground conditions; however, if penetration of the pile equal to the cutting-edge depth (1.0 x CED) in one rotation, the reduction in ultimate resistance can be reduced.

4.3 Comparison of cutting-edge and cone end shape piles

Steel pipe piles with cutting-edge end and cone end were installed by pressing and rotation. The pressing rate and rotation speed were kept similar for both types of piles.

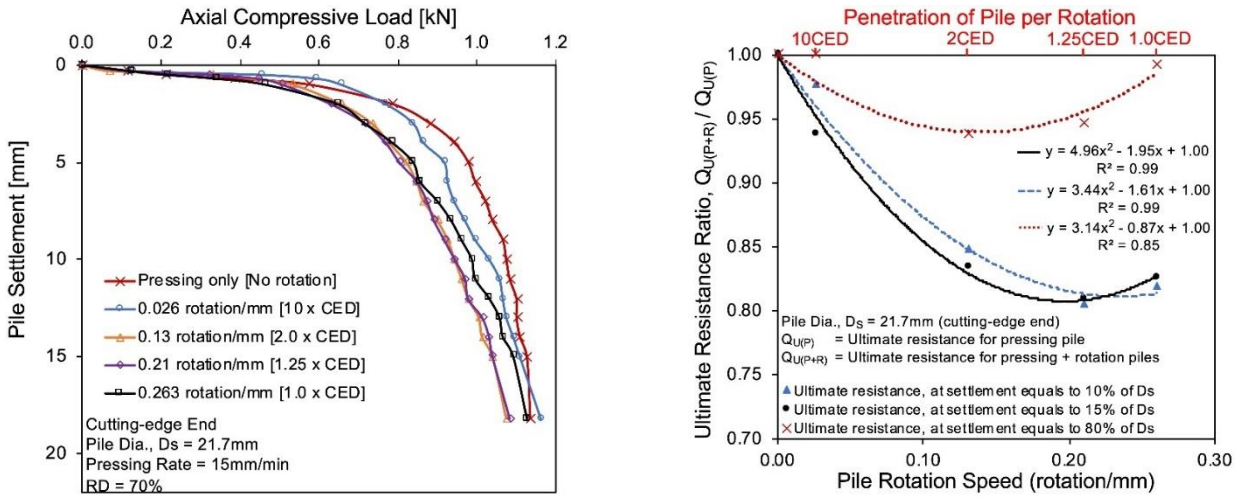

(a) Influence on load settlement response (b) Influence on ultimate resistance

Fig. 9 Ultimate resistance of cutting-edge end pile at different rotation speed and cutting-edge depth

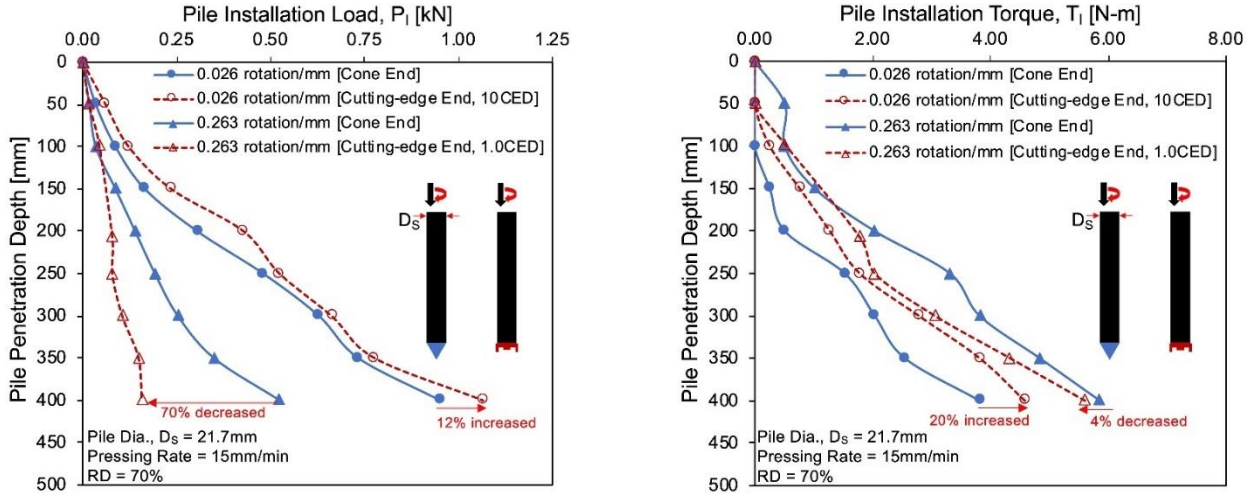

(a) Comparison of installation load (b) Comparison of installation torque

Fig. 10 Comparison of installation effort for cutting-edge and cone end piles

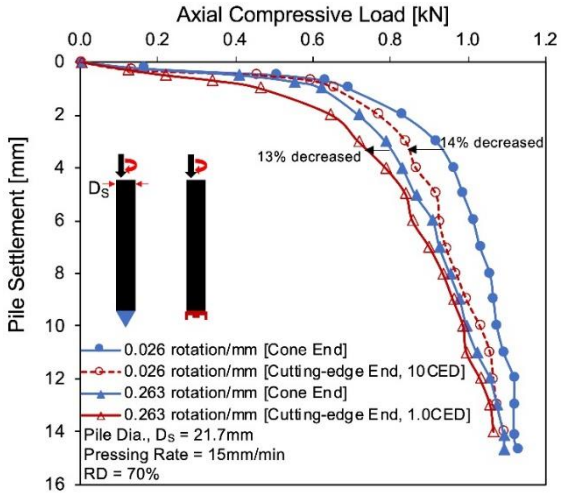

Fig. 11 Comparison of load settlement response of cutting-edge and cone end piles

The loading rate during the pile load test was also kept similar for both types of piles. Test results indicated that the cutting-edge end shaped pile increases the installation load by 12% from the cone end pile at a rotation speed of 0.026

rotation/mm (10 x CED). However, at a higher rotation speed, i.e., penetration of pile equal to the cutting-edge depth in one rotation (1.0 x CED), the installation load of cutting-edge end shaped pile is reduced by 70% from the cone end pile, as shown in Fig. 10(a). Similarly, the installation torque at a higher rotation speed (1.0 x CED) is reduced by 4% from the cone end pile, as shown in Fig. 10(b). These results indicated that less installation effort (load and torque) is required to install the cutting-edge end pile than the cone end pile if penetration of the pile in one rotation equal to the cutting-edge depth (1.0 x CED).

Test results indicated that the ultimate resistance (considered at the settlement of 15% of pile diameter) of cone end pile is 13~14% higher than the cutting-edge end pile at similar rotation speeds, as shown in Fig. 11. However, at the plunging resistance state, the load settlement curves for both types of piles approaching a common value, as shown in Fig. 11.

5. Conclusions

This paper investigates the effect of end shape and pile rotation on the installation effort (load and torque) and ultimate bearing resistance in dense sand. Three types of pile end shapes such as, flat end, cone end, and cutting-edge end, are considered in this study. Model piles are installed in the model ground by pressing and simultaneously pressing and rotation methods. The pressing rate is kept constant throughout the study, whereas rotation speed is varied. Based on the test results, the following conclusions are drawn,

• In the pressing method of installation, the cone end pile required the least installation load to install the pile in dense sand. Moreover, the ultimate resistance of cone end pile is higher than the flat end and cutting-edge end piles. This increase in the ultimate resistance of the cone end pile is due to the ground densification below the pile tip.

• In the case of cutting-edge end pile installation (involving simultaneous pressing and rotation), test results indicated that installation load decreased with an increase in rotation speed. At the same time, installation torque increased with an increase in rotation speed. The results also showed that installation effort (load and torque) could be reduced or minimized if penetration of the pile in one rotation equals the cutting-edge depth, i.e., 1.0 x CED. An empirical relationship (Eq. (3)) between installation load, penetration of pile per rotation, torque, and rotation speed is also presented in this study. Moreover, it is observed that rotation speed reduces the ultimate resistance of pile in dense ground conditions. However, if penetration of the pile equal to the cutting-edge depth (1.0 x CED) in one rotation, then the reduction in ultimate resistance can be reduced.

• In this study, the comparison between cone end and cutting-edge end piles in dense sand indicated that cutting-edge end pile required the least installation effort (load and torque) when penetration of the pile in one rotation equal to the cutting-edge depth (1.0 x CED). Moreover, the ultimate resistance at the plunging resistance state is more or less similar for both types of piles. Therefore, in order to reduce the installation effort, it is suggested to use a cutting-edge end pile.

Acknowledgments

The first author acknowledges the Asian Development Bank's Japan Scholarship Program (ADB-JSP) for its support by providing the scholarship for this research.

References

Arroyo, M., Butlanska, J., Gens, A., Calvetti, F. and Jamiolkowski, M. (2011), "Cone penetration tests in a virtual calibration chamber", *Geotechnique*, **61**(6), 525-531. https://doi.org/10.1680/geot.9.P.067.

Arshad, M.I., Tehrani, F.S., Prezzi, M. and Salgado, R. (2014), "Experimental study of cone penetration in silica sand using digital image correlation", *Geotechnique*, **64**(7), 551-569. https://doi.org/10.1680/geot.13.P.179.

ASTM D1143/D1143M (2007), Standard test methods for deep foundations under static axial compressive load, ASTM International, West Conshohocken, Pennsylvania, U.S.A.

Bolton, M.D., Gui, M.W., Garnier, J., Corte, J.F., Bagge, G., Laue, J. and Renzi, R. (1999), "Centrifuge cone penetration tests in sand", *Geotechnique*, **49**(4), 543-552. https://doi.org/10.1680/geot.1999.49.4.543.

Brucy, F., Meunier, J. and Nauroy, J.F. (1991), "Behavior of pile plug in sandy soils during and after driving", *Proceeding of the 23rd Annual Offshore Technology Conference*, Houston, Texas, U.S.A., May.

Budhu, M. (2010), *Soil Mechanics and Foundations*, 3rd Edition, John Wiley & Sons, Inc., New Jersey, U.S.A.

Daryaei, R., Bakroon, M., Aubram, D. and Rackwitz, F. (2020), "Numerical evaluation of the soil behavior during pipe-pile installation using impact and vibratory driving in sand", *Soil Dyn. Earthq. Eng.*, **134**, 1-15. https://doi.org/10.1016/j.soildyn.2020.106177.

Dickin, E.A. and Leung, C.F. (1983), "Centrifugal model tests on vertical anchors plates", *J. Geotech. Eng.*, **109**(12), 1503-1525. https://doi.org/10.1061/(ASCE)0733-9410(1983)109:12(1503).

Fattah, M.Y., Salim, N.M. and Al-Gharrawi, A.M.B. (2018), "Incremental filling ratio of pipe pile groups in sandy soil", *Geomech. Eng.*, **15**(1), 695-710. https://doi.org/10.12989/gae.2018.15.1.695.

Flynn, K.N. and McCabe, B.A. (2019), "Driven cast-in-situ piles installed using hydraulic hammers: Installation energy transfer and drivability assessment", *Soils Found.*, **59**(6), 1946-1959. https://doi.org/10.1016/j.sandf.2019.09.003.

Frick, D., Schmoor, K.A., Gutz, P. and Achmus, M. (2018), "Model testing of rotary jacked open ended tubular piles in saturated non-cohesive soil", *Proceedings of the 9th International Conference on Physical Modelling in Geotechnics*, London, U.K., July.

Ha, D., Abdoun, T.H., O'Rourke, M.J., Symans, M.D., O'Rourke, T.D., Palmer, M.C. and Stewart, H.E. (2008), "Buried high-density polyethylene pipelines subjected to normal and strike-slip faulting – a centrifuge investigation", *Can. Geotech. J.*, **45**(12), 1733-1742. https://doi.org/10.1139/T08-089.

Heins, E., Bienen, B., Randolph, M.F. and Grabe, J. (2020), "Effect of installation method on static and dynamic load test response for piles in sand", *Int. J. Phys. Model. Geotech.*, **20**(1), 1-23. https://doi.org/10.1680/jphmg.18.00028.

Ishihara, Y. and Haigh, S. (2018), "Cambridge-Giken collaborative working on pile-soil interaction mechanisms", *Proceedings of the 1st International Conference on Press-in Engineering*,

Kochi, Japan, September.
Ishihara, Y., Haigh, S. and Bolton, M. (2015), "Estimating base resistance and N value in rotary press-in", *Soils Found*., **55**(4), 788-797. https://doi.org/10.1016/j.sandf.2015.06.011.
Klos, J. and Tejchman, A. (1981), "Bearing capacity calculation for pipe piles" *Proceedings of 10th International Conference on Soil Mechanics and Foundation Engineering*, Stockholm, Sweden, June.
Kumara, J.J., Kurashina, T. and Kikuchi, Y. (2016), "Effects of pile geometry on bearing capacity of open-ended piles driven into sands", *Geomech*. *Eng*., **11**(3), 385-400. https://doi.org/10.12989/gae.2016.11.3.385.
Lee, J., Salgado, R. and Paik, K. (2003), "Estimation of the load capacity of pipe piles in sand based on cone penetration test results", *J*. *Geotech*. *Geoenviron*. *Eng*., **129**(5), 391-403. https://doi.org/10.1061/(ASCE)1090-0241(2003)129:6(391).
Liu, C., Tang, X., Wei, H., Wang, P. and Zhao, H. (2020), "Model tests of jacked-pile penetration into sand using transparent soil and incremental particle image velocity", *KSCE J*. *Civ*. *Eng*., **24**, 1128-1145. https://doi.org/10.1007/s12205-020-1643-4.
Lu, S.S. (1985), "Pile driving practice in China", *Proceedings of the International Symposium on Penetrability and Drivability of Piles*, San Francisco, California, U.S.A., August.
Malik, A.A. and Kuwano, J. (2020), "Single helix screw pile behavior under compressive loading/unloading cycles in dense sand", *Geotech*. *Geol*. *Eng*. https://doi.org/10.1007/s10706-020-01385-4.
Malik, A.A., Kuwano, J., Tachibana, S. and Maejima, T. (2019), "Effect of helix bending deflection on load settlement behaviour of screw pile", *Acta Geotechnica*, **14**(5), 1527-1453. https://doi.org/10.1007/s11440-019-00778-x.
Mao, W., Aoyama, S. and Towhata, I. (2020), "A study on particle breakage behavior during pile penetration process using acoustic emission source location", *Geosci*. *Front*., **11**(2), 413-427. https://doi.org/10.1016/j.gsf.2019.04.006.
Massarsch, K.R. and Wersall, C. (2013), "Cumulative lateral soil displacement due to pile driving in soft clay", *Proceedings of the Geo-Congress 2013*, San Diego, California, U.S.A., March.
McCammon, N.R. and Golder, H.Q. (1970), "Some loading tests on long pipe piles" *Geotechnique*, **20**(2), 171-184. https://doi.org/10.1680/geot.1970.20.2.171.
Melnikov, A.V. and Boldyrev, G.G. (2014), "Experimental study of sand deformations during CPT", *Proceedings of the 3rd International Symposium on Cone Penetration Testing*, Las Vegas, U.S.A., May.
Nagai, H., Tsuchiya, T. and Shimada, M. (2018), "Influence of installation method on performance of screwed pile and evaluation of pulling resistance", *Soils Found*., **58**(2), 355-369. https://doi.org/10.1016/j.sandf.2018.02.006.
Ni, P., Mangalathu, S., Mei, G. and Zhao, T. (2017), "Permeable piles: An alternative to improve the performance of driven piles", *Comput*. *Geotech*., **84**, 78-87. https://doi.org/10.1016/j.compgeo.2016.11.021.
Ovesen, N.K. (1981), "Centrifuge tests of the uplift capacity of anchors", *Proceedings of the 10th International Conference on Soil Mechanics and Foundation Engineering*, Stockholm, Sweden, June.
Paik, K., Salgado, R., Lee, J. and Kim, B. (2003), "Behavior of open- and close-ended piles driven into sands", *J*. *Geotech*. *Geoenviron*. *Eng*., **129**(4), 296-306. https://doi.org/10.1061/(ASCE)1090-0241(2003)129:4(296).
Paikowsky, S.G. and Whitman, R.V. (1990), "The effects of plugging on pile performance and design", *Can*. *Geotech*. *J*., **27**(4), 429-440. https://doi.org/10.1139/t90-059.
Phuong, N.T.V., Van Tol, A.F., Elkadi, A.S.K. and Rohe, A. (2016), "Numerical investigation of pile installation effects in sand using material point method", *Comput*. *Geotech*., **73**, 58-71. https://doi.org/10.1016/j.compgeo.2015.11.012.
Randolph, M.F., Dolwin, J. and Beck, R. (1994), "Design of driven piles in sand", *Geotechnique*, **44**(3), 427-448. https://doi.org/10.1680/geot.1994.44.3.427.
Randolph, M.F., Steinfelt, J.S. and Worth, C.P. (1979), "The effect of pile type on design parameters for driven piles", *Proceedings of the 7th European Conference on Soil Mechanics*, London, U.K., September.
Sharif, Y.U., Brown, M., Ciantia, M.O., Cerfontaine, B., Davidson, C., Knappett, J., Johannes, M. and Ball, J.D. (2020), "Using DEM to create a CPT based method to estimate the installation requirements of rotary installed piles in sand", *Can*. *Geotech*. *J*. https://doi.org/10.1139/cgj-2020-0017.
Smith, I.M., To, P. and Wilson, S.M. (1986), "Plugging of pipe piles", *Proceedings of the 3rd International Conference on Numerical Method in Offshore Piling*, Nantes, France, May.
Sun, G., Hasanipanah, M., Amnieh, H.B. and Foong, L.K. (2020), "Feasibility of indirect measurement of bearing capacity of driven piles based on a computational intelligence technique", *Measurement*, **156**, 1-10. https://doi.org/10.1016/j.measurement.2020.107577.
Truong, P. and Lehane, B.M. (2018), "Effects of pile shape and pile end condition on the lateral response of displacement piles in soft clay", *Geotechnique*, **68**(9), 794-804. https://doi.org/10.1680/jgeot.16.P.291.
White, D.J., Deeks, A.D. and Ishihara, Y. (2010), "Novel piling: Axial and rotary jacking", *Proceedings of the 11th International Conference on Geotechnical Challenges for Urban Regeneration*, London, U.K., January.
Yang, J. (2006), "Influence zone of end bearing piles in sand", *J*. *Geotech*. *Geoenviron*. *Eng*., **132**(9), 1229-1237. https://doi.org/10.1061/(ASCE)1090-0241(2006)132:9(1229).
Yang, S., Liu, J., Garg, A. and Zhang, M. (2020), "Analytical solution for estimating bearing capacity of a closed soil plug: Verification using an on-site static pile test", *J*. *Mar*. *Sci*. *Eng*., **8**(7), 1-12. https://doi.org/10.3390/jmse8070490.
Yang, Z.X., Jardine, R.J., Zhu, B.T., Foray, P. and Tsuha, C.H.C. (2010), "Sand grain crushing and interface shearing during displacement pile installation in sand", *Geotechnique*, **60**(6), 469-482. https://doi.org/10.1680/geot.2010.60.6.469.

CC